Korean J. Chem. Eng., 34(11), 2984-2992 (2017)
DOI: 10.1007/s11814-017-0204-0

pISSN: 0256-1115
eISSN: 1975-7220

Solar photocatalytic decolorization of synthetic dye solution using pilot scale slurry type falling film reactor

Sarangapany Saran, Gangarapu Manjari, Patchaiyappan Arunkumar, and Suja Purushothaman Devipriya†

Environmental Photocatalysis Research Laboratory, Department of Ecology and Environmental Sciences, Pondicherry University, Pondicherry 605014, India
(*Received 21 March 2017 • accepted 24 July 2017*)

Abstract−Ag deposited TiO_2 was prepared by simple chemical reduction method and its photocatalytic efficiency was evaluated for the decolorization of methylene blue dye using pilot scale slurry type falling film reactors (FFR) under sunlight. The characterization of the prepared catalysts by XRD, TEM, EDAX, DRS and PL confirmed that silver, which acts as electron trap, was deposited over the TiO_2 surface. The operational parameters, such as catalyst loading, concentration of the dye solution, pH of the slurry, addition of oxidizing agents and effect of different substrates, were optimized. The photocatalytic efficiency of Ag deposited TiO_2 increased two-fold times than pure TiO_2 and the maximum decolorization of dye was observed under acidic conditions. The reaction rate significantly increased with the addition of oxidizing agent H_2O_2. The ceramic tile as well as double skin reactor have higher photocatalytic efficiency than glass as substrate. In addition, Ag-deposited TiO_2 photocatalyst could be easily recovered by simple sedimentation process and reused for repeated experimental cycles with more than 95% decolorization efficiency.

Keywords: Falling Film Reactor, Solar Photocatalysis, Ag Deposited TiO_2, Dye Decolorization

INTRODUCTION

Synthetic dyes are toxic, recalcitrant chemical compounds, potentially carcinogenic and mutagenic in nature, hazardous to human health and environment [1,2]. Industries such as textile, carpet, printing, paper and food industries are the major consumers of these dye stuffs while they discharge their effluent directly into the water bodies such as rivers, lakes, ponds without any treatment [3,4]. It has been reported that reactive dyes from industrial azo dye houses are responsible for almost 30% of water pollution due to its effluent discharge [5]. The untreated colored wastewater is toxic to plants and microorganisms and blocks the light penetration, thereby decreasing the photosynthesis and raising the chemical oxygen demand (COD) in the aquatic ecosystem [6,7]. Hao et al. [8] reported that cationic dyes are more toxic than anionic dyes. Sulfonated azo compounds in dye effluents typically resist biodegradation and are either precipitated with the sewage sludge or discharged into rivers [9]. Conventional methods used in the treatment of dye wastewater such as flocculation, coagulation, adsorption using activated carbon and biological treatments have certain limitations. In biological processes, azo bond present in the dyes is transferred to aromatic compounds, which is carcinogenic and more hazardous than dyes [10]. Whereas, adsorption using activated carbon, transfers the pollutants from one phase to other phase, i.e., from liquid phase to solid phase, whereas coagulation and flocculation produce more sludge, which is tough to treat and dispose [11].

In this context, titanium dioxide (TiO_2) mediated photocatalysis is emerging as an alternative tool to degrade dye pollutants, as it is nontoxic, cheap, abundant, thermal and photo stable [12,13]. The main drawbacks associated with TiO_2 photocatalysis are fast e^- and h^+ recombination rate and requirement of near ultra violet (UV) spectra to initiate the charge separation process, which limits its practical application [14]. To overcome these difficulties, doping or decorating noble metals over TiO_2 surface is gaining importance as its decreases the electron hole recombination rate by acting as electron quencher and also due to surface plasmon resonance property, which increases the generation of reactive oxygen species (ROS) under visible region [15,16]. Among the various noble metals, silver (Ag) is popular due to cost efficiency, easy availability and its high stocky barrier [17,18]. When Ag deposited TiO_2 catalyst is exposed to sunlight, it induces the charge separation process, which excites an electron from valence band to conduction band, subsequently leaving a hole in the valence band [19]. The conduction band electron is trapped by the silver ions present in the surface of TiO_2, thereby decreasing the electron (e^-) and hole (h^+) recombination rate [20,21]. As a result, the surface bound hole reacts with water and oxidizes it into hydroxyl radicals ($^{\bullet}OH$), whereas the electron reduces the molecular oxygen to superoxide radicals which degrade the dye molecules (Fig. 1).

Several literatures report on material preparation and its modifications in order to increase the photocatalytic efficiency using bench scale reactors under controlled conditions [22-24]. Sahoo et al. [25] demonstrated the photocatalytic degradation of Methyl Red dye using Ag doped TiO_2 under UV irradiation. Whereas, Sakthivel et al. [26] studied the efficiency of Pt, Au and Pd deposited on TiO_2 to enhance its photocatalytic activity for the degradation of Acid Green 16 dye using high pressure mercury vapor lamp. But, the treatment of dye wastewater in large volume under sunlight using

†To whom correspondence should be addressed.
E-mail: devipriyasuja@gmail.com, suja.ees@pondiuni.edu.in

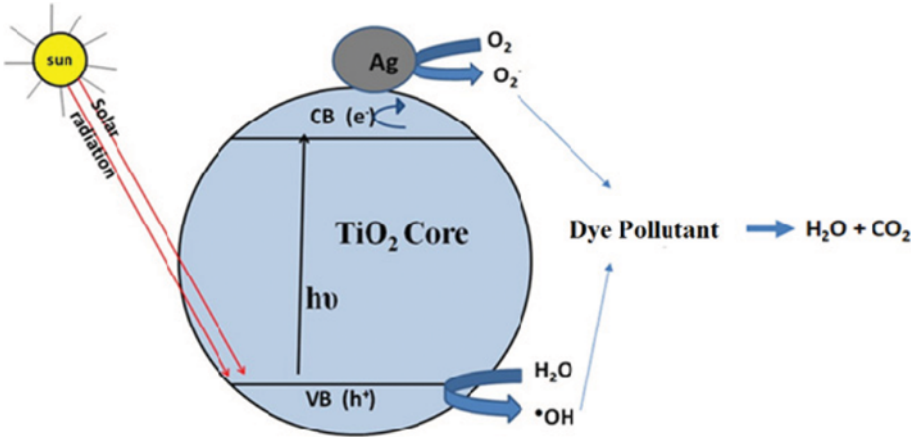

Fig. 1. Mechanisim of Ag deposited TiO_2 photocatalysis.

pilot scale reactors is very much limited.

Hence from this perspective, we mainly studied the photocatalytic decolorization of synthetic dye solution using a non-concentrating falling film slurry reactor under sunlight. In this study, a cost-effective pilot scale reactor was developed for photocatalytic decolorization of methylene blue, selected as a model pollutant. The effects of various operational parameters such as catalyst loading, initial dye concentration, initial slurry pH, and addition of hydrogen peroxide (H_2O_2) etc., were studied. The solar photocatalytic efficiency of two different substrates, glass and tiles, used in the reactors was validated.

EXPERIMENTS

1.Chemicals

Titanium dioxide (TiO_2), silver nitrate ($AgNO_3$), sodium borohydride ($NaBH_4$), hydrogen peroxide 25% v/v (H_2O_2), sulfuric acid (H_2SO_4) and sodium hydroxide (NaOH) were received from Merck Chemicals (India) with analytic grade and used without further purification. Methylene blue, $C_{16}H_{18}ClN_3S$ (C.I. 52015, MW- 319.85) was purchased from Merck India Ltd., with 99% purity and its chemical structure is shown in Fig. 2.

2. Preparation of Ag Decorated TiO_2 by Chemical Reduction Method

Using simple chemical reduction method Ag deposited TiO_2 (1.0 wt%) was prepared by dispersing 5 g of TiO_2 in 100 ml of distilled water by sonication. Under constant stirring 5 ml of 0.1 mole $AgNO_3$ solution was added followed by addition of 5 ml of 0.1 mole of $NaBH_4$ as reducing agent. The resultant mixture was further dried in hot air oven at 120 °C overnight and the product

Fig. 2. Structure of methylene blue dye.

obtained was calcined at 400 °C for 3 hours, cooled and used [27].

3. Characterization of Prepared Particles

The X-ray diffraction (XRD) pattern of pure and Ag deposited TiO_2 was measured by using powder PAN analytical X-ray diffractometer between 20° to 80°. The average crystallite size (D in nm) of prepared particles was determined from XRD patterns using Scherrer's equation by the following equation.

$$D=k\lambda/\beta\cos\theta \quad (1)$$

where, k is a constant equal to 0.9; λ, the X-ray wavelength equal to 0.154 nm; β is the full width at half maximum, and θ is the half diffraction angle. Scanning electron microscope (SEM- Hitachi, Model: S-3400 N) was used to measure the surface morphology of the particles, and the elemental mapping was by using ThermoSuperDry II make energy dispersive X-ray spectroscopy (EDAX) attached to the SEM. The size and shape of the prepared particles were determined using Philips CM-10 High resolution transmission electron microscopy. Diffuse reflectance spectra (DRS) were recorded with Varian Cary 5000 UV-Vis. NIR spectrophotometer using $BaSO_4$ as the reference. The Brunauer-Emmett-Teller (BET) surface area of the particles was measured by nitrogen gas adsorption-desorption method using ASAP 2010, Micromeritics. The samples were degassed at 150 °C for 3 h under the vacuum condition to remove the moisture. The photoluminescence (PL) emission spectra were measured with JY Fluorolog - FL3-11 make spectrofluorometer.

4. Fabrication of Pilot Scale Non Concentrating Falling Film Photoreactor

The pilot scale non-concentrating slurry type falling film reactor was fabricated either with tiles or a glass sheet with an illumination surface of about 60×120 cm mounted on a fixed platform tilted at 35° (local latitude), as shown in Fig. 3(a) Glass substrate and (b) Ceramic tile substrate reactor. A peristaltic pump powered by 35 W solar photovoltaic cells was used to recirculate the dye solution mixed with the catalyst from the tank to the reactor by spraying through a perforated manifold over the substrate.

5. Photocatalytic Decolorization Studies

The photocatalytic experiments were conducted on the pilot scale non-concentrating falling film slurry type photo catalytic reactors

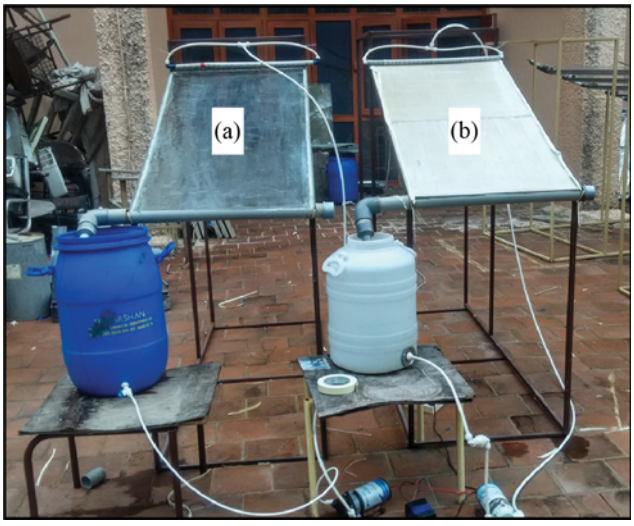

Fig. 3. Image of slurry type falling film reactor (a) glass substrate and (b) ceramic tile substrate.

operated with 25 L of synthetic dye wastewater. Dye solutions were prepared with tap water from the laboratory. Control experiments were performed along the side with pure TiO_2 and by direct photolysis, i.e., without any catalyst. All the experiments were on the roof top of our laboratory at Pondicherry University, India, (Local latitude 12.01°N & longitude 79.85°E) under sunlight during the months of April to July 2016, between 10.00 a.m. to 2.00 p.m. By using UV tech, a handheld radiometer, the average solar intensity was measured with 365 nm sensor. The experiment was conducted under the dark condition for 30 min to establish adsorption/desorption equilibrium with the catalyst and dye by covering the reactor with a black cover. For photocatalytic experiments, the cover was removed from the photo reactors which were exposed to sunlight for 120 min to check the efficiency of the prepared catalysts. At specific intervals, 3 mL of samples was collected and filtered using 0.22 micron Millipore membrane, and the filtrate was used for the determination of color removal using spectrophotometric method by measuring λ_{max} value at 661 nm for MB. The evaporation loss on the volume of water was adjusted by adding the required amount of distilled water before each subsequent experiment. The experiments were repeated thrice and the results were averaged. The percentage colour removal was calculated by using the following equation:

$$\text{Colour removal } \% = \frac{C_o - C_t}{C_o} \times 100 \quad (2)$$

where C_o is the initial concentration of dye and C_t is dye concentration at different time t. Influence of operational parameters such as different catalyst concentration, initial slurry pH, and addition of oxidizing agent, effect of different substrates and reusability of the catalyst was also studied.

RESULTS AND DISCUSSION

1. Characterization Result

XRD pattern of TiO_2 (Fig. 4) confirms the different diffraction

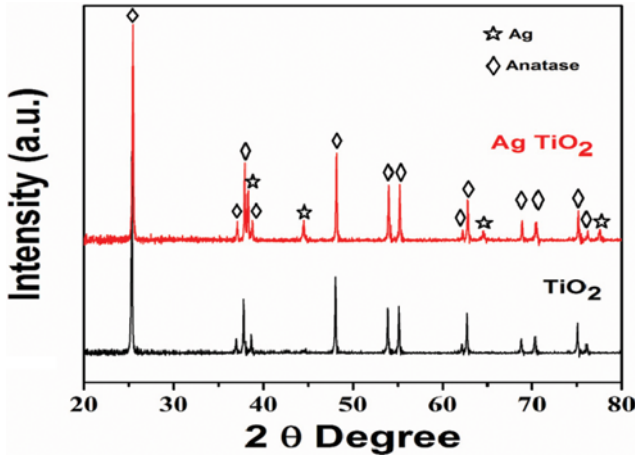

Fig. 4. X-ray diffraction pattern of pure TiO_2 and Ag decorated TiO_2.

planes of anatase phase alone by showing peaks at 25.4°, 37.8°, 48.07°, 54°, 55°, 62.7°, 75.09° (JCPDS reference code: 01-073-1764) and no other planes were observed. The average particle size (D in nm) determined using Scherrer's equation from (101) peak of anatase TiO_2 at 2θ=25.4, was about 49 nm. Whereas, the XRD pattern confirms the presence of Ag in face centric cubic (fcc) over TiO_2 by showing peaks at 2θ of 38.27°, 44.45°, 64.6° and 77.5° (JCPDS reference code:01-087-0718). The average crystallite size of Ag deposited TiO_2 is about 54 nm, the particle size slightly increased due to the covering of Ag over the TiO_2 surface and also calcination effect [28,29].

The optical properties of pure and Ag deposited TiO_2 were studied by using UV-Vis. Spectrophotometer to measure the diffused reflectance spectra (DRS). Fig. 5 depicts pure TiO_2 and Ag deposited TiO_2, whereas pure TiO_2 shows increasing absorbance at UV region due to the optical band gap of TiO_2 [30] and Ag deposited TiO_2 shows a broad band absorption under visible region that is attributed to the surface plasmon resonance properties of silver nanoparticles deposited over the TiO_2, which produces more ROS [31,32].

The morphology and size of pure TiO_2 and Ag deposited TiO_2

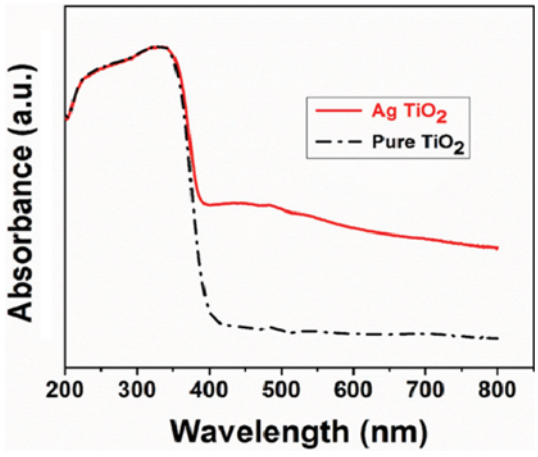

Fig. 5. UV-vis. Absorption spectra of pure and Ag decorated TiO_2.

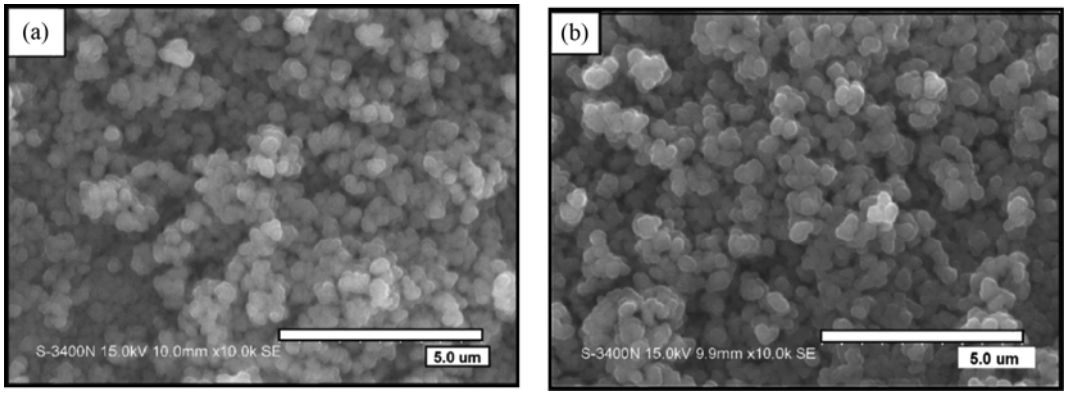

Fig. 6. SEM image of (a) pure and (b) Ag decorated TiO_2.

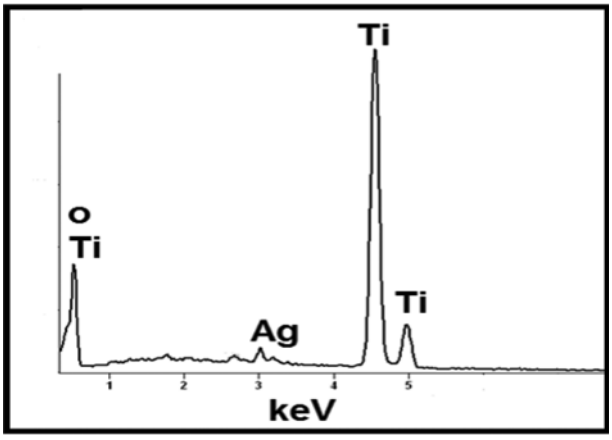

Fig. 7. EDAX spectra of Ag decorated TiO_2.

were measured by using SEM and TEM. SEM images of both the particles have similar morphology: spherical with agglomerated structure (Fig. 6(a) and (b)). The elemental composition of pure TiO_2 and Ag deposited TiO_2 was confirmed through SEM equipped EDAX (Fig. 7). It shows the spectral signal of elemental silver, titanium and oxygen, indicating the deposition of Ag over TiO_2 surface. TEM micrographs of pure TiO_2 and Ag deposited TiO_2 were irregular in shape and size with slight difference in morphological features (Fig. 8(a) and (b)). Fig. 8(b) shows silver nanoparticles with 12-18 nm in size heterogeneously dispersed over the surface of the TiO_2, owing to low silver concentration used for deposition [33].

The BET specific surface area results of the pure TiO_2 and Ag deposited TiO_2 were about 11.8 m^2/g and 9.2 m^2/g, respectively. Ag deposited TiO_2 has less surface area than pure due to the covering of capillaries and hole of the TiO_2 surface with Ag ions [34,35].

The PL emission spectra for both the pure and Ag deposited TiO_2 excited at 330 nm are illustrated in Fig. 9. The results indicate that both emission spectra are similar to each other and exhibit two emission peaks. The first peak at 375 nm is assigned to 3.3 e.v. which is equal to its band gap energy, and the peak at 435 nm matches up with 2.9 ev., attributed to free excitation of O^{2-} charge transfer transition, respectively [36]. The PL spectra of Ag deposited TiO_2 show lesser intensity than pure TiO_2 under the same excitation irradiation, which ensures the reduction in e^- and h^+ recombination rate. Ag nanoparticles have higher metal work function than that of pure TiO_2, so the photogenerated conduction band electrons in TiO_2 surface will transfer to Ag, which acts as electron acceptor. From the results, it is inferred that photocatalytic efficiency is enhanced with reduction in photogenerated e^- and h^+ recombination rate [37,38].

2. Solar Photocatalytic Decolorization of Methylene Blue Dye Using Slurry Type Falling Film Reactor

The efficiency of the prepared particles was evaluated by select-

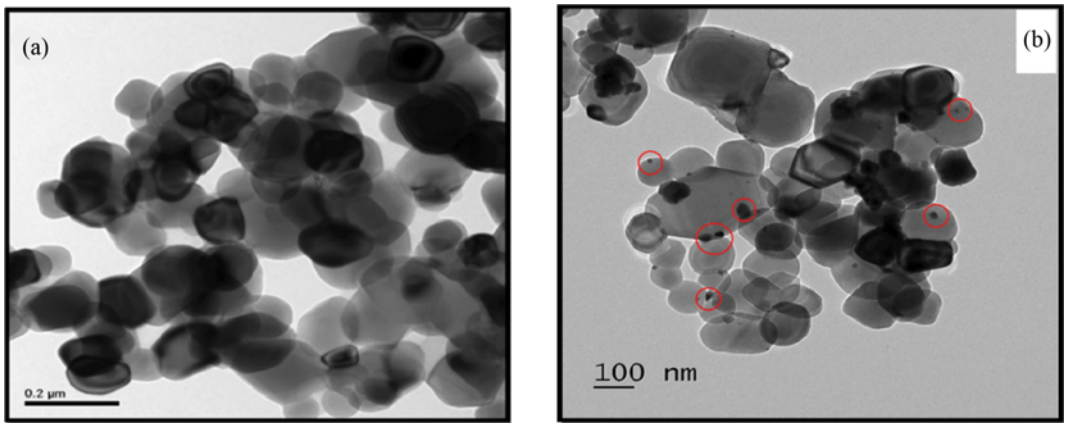

Fig. 8. TEM image of (a) pure TiO_2 and (b) Ag decorated TiO_2.

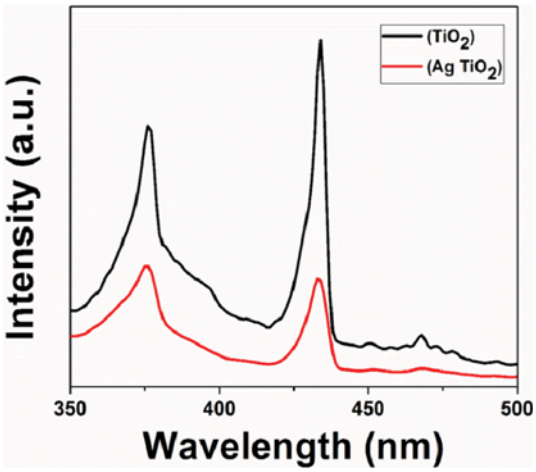

Fig. 9. PL spectra of pure TiO_2 and Ag decorated TiO_2.

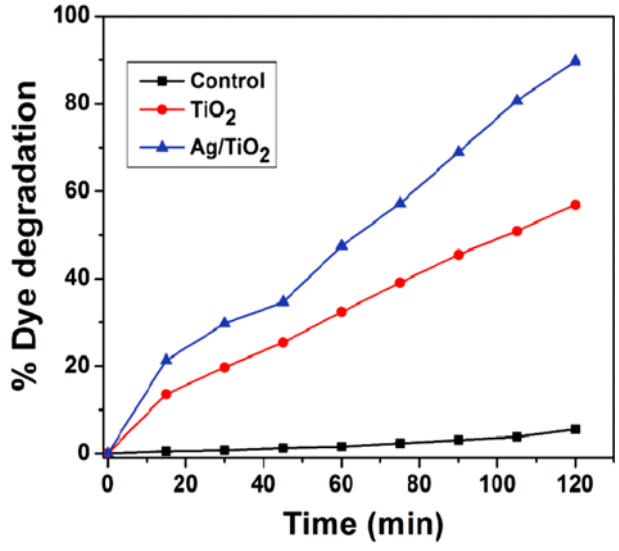

Fig. 10. Solar photocatalytic methylene blue dye degradation (Dye conc.-10 ppm; catalyst conc.-100 ppm; flow rate-30 L h^{-1}; pH-6.0; solar intensity-1.1 mW/cm^2; substrate-tiles; time-120 mins).

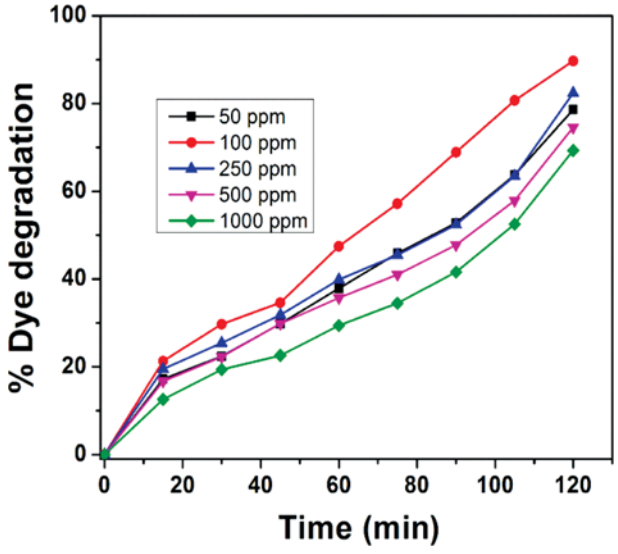

Fig. 11. Effect of different initial catalyst concentration on MB dye degradation (Dye conc.-10 ppm; flow rate-30 L h^{-1}; pH-6.0; solar intensity-1.1 mW/cm^2; substrate-tiles; time-120 mins).

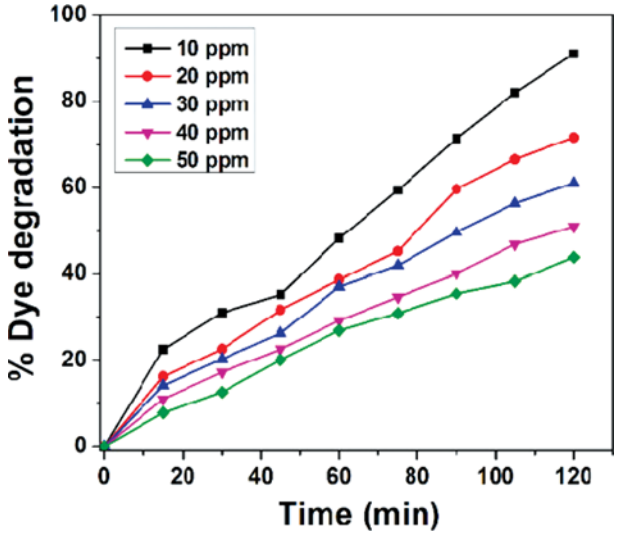

Fig. 12. Effect of different initial dye concentration on MB dye degradation (Catalyst conc.-10 ppm; flow rate-30 L h^{-1}; pH-6.0; solar intensity-1.1 mW/cm^2; substrate-tiles; time-120 mins).

ing methylene blue dye as model pollutant. Each reactor was operated in batch recycle mode with 25 liters of dye mixed with various catalysts in slurry mode, by passing it over the tile substrate as a thin film. The experiment was performed with pure, Ag decorated TiO_2 and by direct photolysis as illustrated in Fig. 10. The results show that pure TiO_2 is less efficient to decolorize MB dye, about 57%, due to weak adsorption under visible region [39]. Whereas, Ag decorated TiO_2 shows nearly two-fold increase in photocatalytic decolorization activity of about 90% due to electron quenching ability of silver, which reduces the e^- and h^+ recombination rate, thereby increasing the production of more ROS under same operating conditions. Negligible reduction of about 5.6% was observed by direct photolysis [40]. Since Ag deposited TiO_2 shows higher decolorization than pure one, the remaining experiments were conducted with Ag decorated TiO_2 alone to optimize the reaction parameters.

2-1. Effect of Catalyst Concentration on Dye Decolorization

Effect of different catalyst loading has profound influence on dye decolorization rate, which was evaluated using Ag deposited TiO_2 ranging from 50 ppm to 1,000 ppm in order to optimize the catalyst concentration. Fig. 11 shows the percentage decolorization of MB dye after 120 min under sunlight. A gradual increase in the decolorization up to 100 ppm is observed and further increase in catalyst concentration leads to decrease in decolorization rate as reported earlier by Wetchakun et al. [41] and Devadi et al. [42]. Initial increase in dye decolorization was due to increase in number of active sites with increasing amount of catalyst surface, which in turn produced more ROS. Further increase with catalyst con-

centration may increase the turbidity, which hinders the penetration of sun light through screening effect [43].

2-2. Effect of Initial Dye Concentration

The initial dye concentration has a pivotal role on decolorization rate. To study the effect of different initial dye concentration on photocatalysis, experiments were conducted with varying initial dye concentration from 10 ppm to 50 ppm with constant catalyst concentration of 100 ppm. Fig. 12 illustrates decolorization percentage with varying dye concentrations. The results show that there was a gradual decrease in photocatalytic decolorization efficacy when the initial dye concentration was increased from 10 ppm to 50 ppm, i.e., about 90% to 44%, respectively, after 2 hours of illumination under sunlight. This is because the catalyst loading remains constant, which produces the same concentration of ROS. Whereas, dye molecules increase with increasing concentration, resulting in insufficient number of ROS for dye decolorization, which decreases the rate of the reaction [44,45].

2-3. Effect of pH of Solution

The initial slurry pH of dye solution may have profound effect on the rate of dye decolorization, as it influences the surface charge of particles. To study this, various experiments were performed by varying the pH range from 2 to 10. Fig. 13 illustrates that the percentage dye decolorization decreases from about 99% to 65% after 120 min under sunlight. Under acidic conditions, TiO_2 surface becomes more positively charged, thereby facilitating more adsorption of the dye and increase in the decolorization rate. Similar results were also observed by Zhang et al. [46] and Wu et al. [47], which elucidates that MB dye gets strongly adsorbed over TiO_2 surface under an acidic condition, which facilitates faster degradation.

2-4. Effect of H_2O_2 Addition

To investigate the effect of addition of H_2O_2, experiments were conducted at varying H_2O_2 concentrations from 0 mM to 10 mM. The results revealed that the rate of color removal increased with increasing concentration of H_2O_2 from 99% to 72% after 2 hours

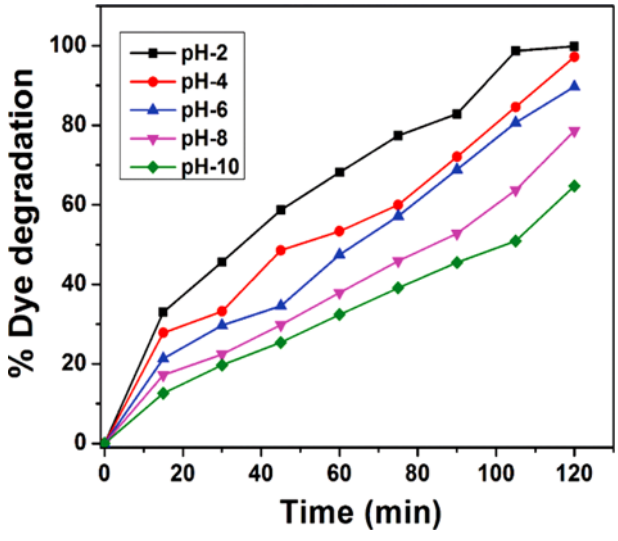

Fig. 13. Effect of initial slurry pH on MB dye degradation (Dye conc.-10 ppm; catalyst Ag/TiO_2-100 ppm; flow rate-30 L h^{-1}; solar intensity-1.1 mW/cm^2; substrate-tiles; time-120 mins).

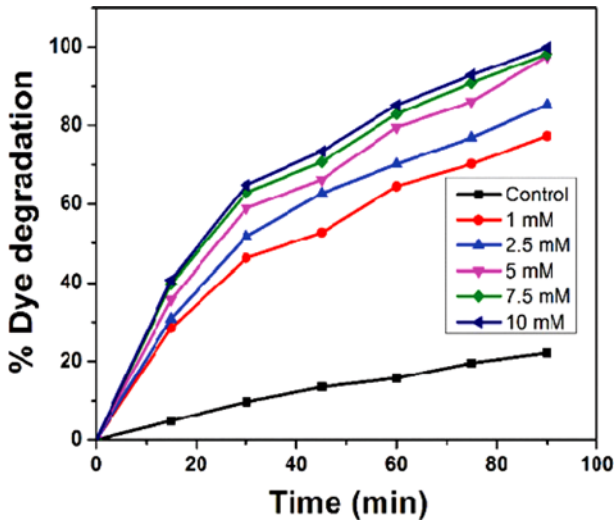

Fig. 14. Effect of addition of H_2O_2 on MB dye degradation (Dye conc.-10 ppm; catalyst Ag/TiO_2-100 ppm; pH-6.0; flow rate-30 L h^{-1}; solar intensity-1.1 mW/cm^2; substrate-tiles; time-90 mins).

exposure under sunlight (Fig. 14). Nearly 22% decolorization of dye was observed when the experiment was performed with addition of 10 mM H_2O_2 alone without catalyst as control. H_2O_2 dissociates into $^{\bullet}OH$ radicals, which is the primary oxidizing agent and also it reduces the e^- and h^+ recombination rate, bringing about faster decolorization rate [29,48]. Saggioro et al. [49] also reported that the photocatalytic decolorization rate increased two-fold on addition of optimum volume of H_2O_2 to the dye solution.

2-5. Effect of Operational Parameters on Dye Decolorization

The reactor was operated with all optimum operational conditions: with 100 ppm catalyst conc., 10 ppm dye, flow rate 30 L h^{-1}, at pH 2 and with 10 mM of H_2O_2 addition, around 99% decolor-

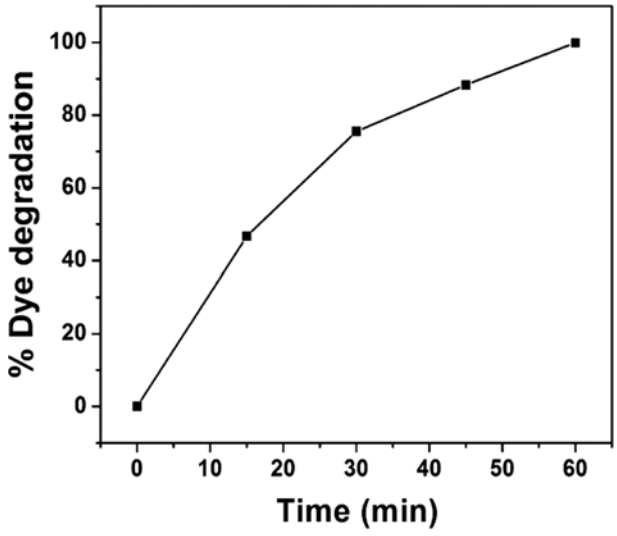

Fig. 15. Effect of optimum operational parameters on MB dye degradation (Dye conc.-10 ppm; catalyst Ag/TiO_2-100 ppm; pH-2.0; flow rate-30 L h^{-1}; solar intensity-1.1 mW/cm^2; substrate-tiles; time-60 mins; H_2O_2 conc.-10.0 mM).

Table 1. Comparison of different pilot scale reactors for the photocatalytic degradation of various wastewater from literature

Pollutant type	Catalyst	Light source	Reactor type	Treatment time (hours)	Degradation %	Reference
4-Chlorophenol water	TiO_2	Sunlight	Slurry Flat plate reactor	2.5	60	[50]
Pretreated landfill leachate	TiO_2	Fluorescent tubes	Immobilized over glass sheet (TFFBR)	8	57	[51]
Synthetic dye water	TiO_2 P25	Sunlight	Immobilized over cement surface (TFFBR)	8	47	[52]
Dichloroacetic acid	TiO_2	Sunlight	Double skin sheet reactor	3.5	100	[53]
Pesticides mixture	TiO_2	Sunlight	Immobilized over Ahlstrom paper (STEP reactor)	4.5	80	[54]
Benzoic acid containing wastewater	Degussa TiO_2 P25	Sunlight	Immobilized stainless steel flat plates (TFFBR)	3	100	[55]
Biologically pretreated industrial wastewater	TiO_2 P25	Sunlight	Double skin sheet reactor	5.5	40	[56]
Secondary treated sugar refinery wastewater	Ag/TiO_2	Sunlight	Immobilized on ceramic surface (TFFPR)	3	99	[33]
Synthetic dye solution	Ag/TiO_2	Sunlight	Slurry (FFR)	1	99	The present study

ization of dye was observed within 60 minutes under 1.1 mW/cm^2 average solar irradiation (Fig. 15). On comparison with several authors, a slurry type falling film reactor was found to be more efficient for the treatment of dye solution (Table 1) [50-56].

2-6. Effect of Different Substrate (Glass vs Tile)

To study the effect of different substrate on dye decolorization, the experiment was performed with glass plate vs ceramic tiles with optimal operation parameters (Fig. 16). Interestingly, tiles show maximum decolorization than glass plates, which was due to non-concentrating solar energy in glass plate than in tiles. In the tile surface, the solar light is reflected by its polished surface, whereas in glass plate the rays penetrate through the glass, which is the possible reason for the reduction in the efficiency than in tiles. There was no significant change in the dye decolorization when the experiment was performed with double skin reactor, i.e., a glass plate was placed over the tile surface with 1 cm gap to prevent water loss by evaporation.

2-7. Reusability of Catalyst

The stability of Ag decorated TiO_2 was evaluated by conducting the experiments in repeated cycles. The catalyst was recovered by simple sedimentation process and dried in hot air oven at 100 °C for 2 hours to remove the moisture and was reused in the next successive cycles. Fig. 17 illustrates the high stability of the catalyst

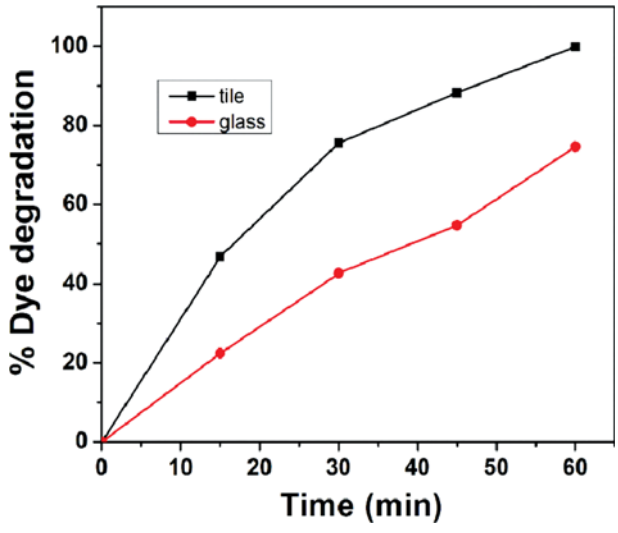

Fig. 16. Effect of different substrate on MB dye degradation (Dye conc.-10 ppm; catalyst Ag/TiO_2-100 ppm; pH-2.0; flow rate-30 L h^{-1}; solar intensity-1.1 mW/cm^2; substrate-tiles; time-60 mins; H_2O_2 conc.-10.0 mM).

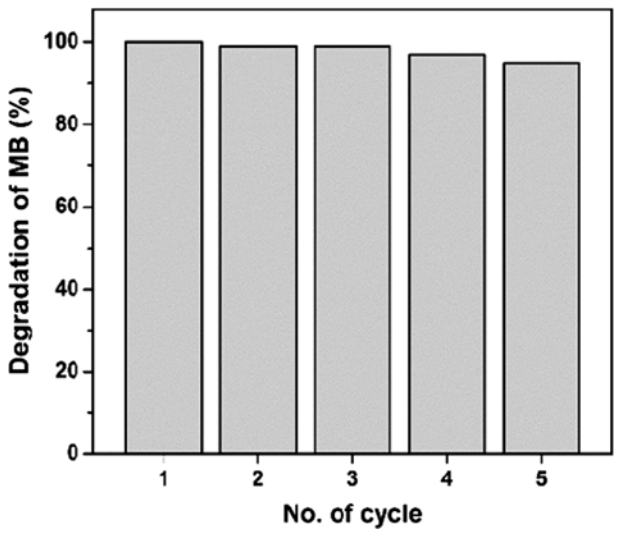

Fig. 17. Repeated reuse of Ag deposited TiO_2 catalyst for MB dye degradation under optimum operational conditions.

even after five repeated cycles.

CONCLUSION

Silver decorated TiO_2 was prepared by a simple chemical reduction method using $NaBH_4$ as reducing agent. Characterization results confirm that TiO_2 decorated with silver extends its wavelength response towards the visible light region and increases the production of ROS by reducing the e^- and h^+ recombination rate. A simple, cost effective fixed angle falling film reactor designed and fabricated locally was studied for dye decolorization. The results show that the decolorization efficiency increased two-fold in Ag-deposited TiO_2 than pure TiO_2. Effects of various operational parameters on dye decolorization were optimized. Ceramic tiles as substrate exhibited high photocatalytic activity compared to glass substrate. The double skin reactor fabricated with transparent glass sheet over the tile surface did not affect the dye decolorization. Such pilot scale falling film reactors are found to be an efficient, cost effective technique for the treatment of various kinds of dye pollutants.

ACKNOWLEDGEMENTS

We acknowledge the University Grants Commission (UGC) India, for funding the major research project (F.No. 40/146/2010 S.R.) and Central Instrumentation Facility (CIF), Centre for Nanoscience and Technology and Department of Earth Sciences, Pondicherry University for characterization studies.

REFERENCES

1. M. A. Habib, I. M. I. Ismail, A. J. Mahmood and M. R. Ullah, *J. Saudi Chem. Soc.*, **16**, 423 (2012).
2. X. Liu, A. Jin, Y. Jia, T. Xia, C. Deng, M. Zhu, C. Chen and X. Chen, *Appl. Surf. Sci.*, **405**, 371 (2017).
3. G. Manjari, S. Saran, T. Arun, A. V. B. Rao and S. P. Devipriya, *J. Saudi Chem. Soc.* (2017), DOI:10.1016/j.jscs.2017.02.004.
4. A. Sandoval, C. Hernández-Ventura and T. E. Klimova, *Fuel*, **138**, 30 (2017).
5. W. Xie, M. Zhang, D. Liu, W. Lei, L. Sun and X. Wang, *ACS Sustain. Chem. Eng.*, **5**, 1392 (2017).
6. A. Vats and S. Mishra, *Environ. Sci. Poll. Res.*, **24**, 11662 (2017).
7. A. Shah, S. Shahzad, A. Munir, M. N. Nadagouda, G. S. Khan, D. F. Shams, D. D. Dionysiou and U. A. Rana, *Chem. Rev.*, **116**, 6042 (2016).
8. O. J. Hao, H. Kim and P. C. Chiang, *Crit. Rev. Environ. Sci. Technol.*, **30**, 449 (2000).
9. D. Mohan, K. P. Singh, G. Singh and K. Kumar, *Ind. Eng. Chem. Res.*, **41**, 3688 (2002).
10. T. Zhang, T. Oyama, A. Aoshima, H. Hidaka, J. Zhao and N. Serpone, *J. Photochem. Photobiol. A Chem.*, **140**, 163 (2001).
11. D. Gümüş and F. Akbal, *Water, Air, Soil Pollut.*, **216**, 124 (2011).
12. A. Patchaiyappan, S. Saran and S. P. Devipriya, *Korean J. Chem. Eng.*, **33**, 2107 (2016).
13. N. Tzikalos, V. Belessi and D. Lambropoulou, *Environ. Sci. Poll. Res.*, **20**, 2305 (2013).
14. H. Wang, S. Dong, Y. Chang and J. L. Faria, *J. Hazard Mater.*, **235**, 230 (2012).
15. S. P. Devipriya, S. Yesodharan and E. P. Yesodharan, *I. J. Photoenergy*, **2012**, Article ID 970474, 1 (2012).
16. M. Abdennouri, A. Elhalil, M. Farnane, H. Tounsadi, F. Z. Mahjoubi, R. Elmoubarki, M. Sadiq, L. Khamar, A. Galadi, M. Baâlala and M. Bensitel, *J. Saudi Chem. Soc.*, **19**, 485 (2015).
17. Z. Chen, L. Fang, W. Dong, F. Zheng, M. Shen and J. Wan, *J. Mater. Chem. A*, **2**, 824 (2014).
18. X. H. Yang, H. T. Fu, X. C. Wang, J. L. Yang, X. C. Jiang and A. B. Yu, *J. Nanopart. Res.*, **16**, 2526 (2014).
19. K. Nakata and A. Fujishima, *J. Photochem. Photobiol. Rev.*, **13**, 169 (2012).
20. B. Yu, K. M. Leung, Q. Guo, W. M. Lau and J. Yang, *Nanotechnol.*, **22**, 115603 (2011).
21. Z. Jiang, W. Wei, D. Mao, C. Chen, Y. Shi, X. Lv and J. Xie, *Nanoscale*, **7**, 784 (2015).
22. J. Colina-Márquez, F. Machuca-Martínez and G. Li Puma, *Environ. Sci. Technol.*, **43**, 8953 (2009).
23. T. Han, Y. Chen, G. Tian, W. Zhou, Y. Xiao, J. Li and H. Fu, *Sci. China Mat.*, **59**, 1003 (2016).
24. L. Karimi, S. Zohoori and M. E. Yazdanshenas, *J. Saudi Chem. Soc.*, **18**, 581 (2014).
25. C. Sahoo, A. K. Gupta and A. Pal, *Desalination*, **181**, 100 (2005).
26. S. Sakthivel, M. V. Shankar, M. Palanichamy, B. Arabindoo, D. W. Bahnemann and V. Murugesan, *Water Res.*, **38**, 3008 (2004).
27. N. Nino-Martinez, G. A. Martinez-Castanon, A. Aragon-Pina, F. Martinez-Gutierrez, J. R. Martinez-Mendoza and F. Ruiz, *Nanotechnol.*, **19**, 065711 (2008).
28. N. Sobana, M. Muruganadham and M. Swaminathan, *J. Mol. Catal. A Chem.*, **258**, 124 (2006).
29. R. J. Tayade, T. S. Natarajan and H. C. Bajaj, *Ind. Eng. Chem. Res.*, **48**, 10262 (2009).
30. Y. Tang, Z. Jiang, Q. Tay, J. Deng, Y. Lai, D. Gong, Z. Dong and Z. Chen, *RSC Adv.*, **2**, 9406 (2012).
31. L. Zhang, J. C. Yu, H. Y. Yip, Q. Li, K. W. K. Wong, A. W. Xu and P. K. Wong, *Langmuir*, **19**, 10372 (2003).
32. E. Liu, L. Kang, Y. Yang, T. Sun, X. Hu, C. Zhu and J. Fan, *Nanotechnol.*, **25**, 165401 (2014).
33. S. Saran, G. Kamalraj, P. Arunkumar and S. P. Devipriya, *Environ. Sci. Poll. Res.*, **23**, 17730 (2016).
34. V. Vamathevan, R. Amal, D. Beydoun, G. Low and S. McEvoy, *J. Photochem. Photobiol. A: Chem.*, **148**, 233 (2002).
35. R. A. Rather, S. Singh and B. Pal, *Sol. Energ. Mat. Sol. Cells*, **160**, 463 (2017).
36. K. Gupta, R. P. Singh, A. Pandey and A. Pandey, *Beilstein J. Nanotechnol.*, **4**, 345 (2013).
37. F. Wu, X. Hu, J. Fan, E. Liu, T. Sun, L. Kang, W. Hou, C. Zhu and H. Liu, *Plasmonics*, **8**, 501 (2013).
38. K. H. Leong, B. L. Gan, S. Ibrahim and P. Saravanan, *Appl. Surf. Sci.*, **319**, 128 (2014).
39. W. Yao, B. Zhang, C. Huang, C. Ma, X. Song and Q. Xu, *J. Mater. Chem.*, **22**, 4050 (2012).
40. A. Ramchiary and S. K. Samdarshi, *Appl. Surf. Sci.*, **305**, 33 (2014).
41. K. Wetchakun, N. Wetchakun and S. Phanichphant, *Desal. Water Treat.*, **57**, 10286 (2016).

42. M. A. H. Devadi, M. Krishna, H. N Murthy and B. S. Sathyanarayana, *Procedia Mater. Sci.*, **5**, 621 (2014).
43. M. R. Sohrabi and M. Ghavami, *J. Hazard. Mater.*, **153**, 1239 (2008).
44. J. Kaur and S. Singhal, *Physica B Condens. Matter.*, **450**, 49 (2014).
45. M. Muruganandham and M. Swaminathan, *J. Hazard. Mater.*, **135**, 86 (2006).
46. T. Zhang, T. Oyama, A. Aoshima, H. Hidaka, J. Zhao and N. Serpone, *J. Photochem. Photobiol. A: Chem.*, **140**, 163 (2001).
47. C. H. Wu and J. M. Chern, *Ind. Eng. Chem. Res.*, **45**, 6450 (2006).
48. B. Neppolian, S. R. Kanel, H. C. Choi, M. V. Shankar, B. Arabindoo and V. Murugesan, *Int. J. Photoenergy*, **5**, 49 (2003).
49. E. M. Saggioro, A. S. Oliveira, T. Pavesi, C. G. Maia, L. F. V. Ferreira and J. C. Moreira, *Molecules*, **16**, 10386 (2011).
50. P. Wyness, J. Klausner, D. Goswami and K. Schanze, *J. Sol. Energy Eng.*, **116**, 7 (1994).
51. M. Bekbolet, M. Linder, D. Weichgrebe and D. Bahnemann, *Sol. Energy*, **56**, 469 (1996).
52. G. Zayani, L. Bousselmi, F. Mhenni and A. Ghrabi, *Desalination*, **246**, 352 (2009).
53. M. Van Well, R. Dillert, D. Bahnemann, V. Benz and M. A. Mueller, *J. Sol. Energy Eng.*, **119**, 119 (1997).
54. H. B. Thu, M. Karkmaz, E. Puzenat, C. Guillard and J. M. Herrmann, *Res. Chem. Intermed.*, **31**, 461 (2005).
55. A. H. C. Chan, C. K. Chan, J. P. Barford and J. F. Porter, *Water Res.*, **37**, 1135 (2003).
56. R. Dillert, A. Cassano, R. Goslich and D. Bahnemann, *Catal. Today*, **54**, 282 (1999).